Proceedings of the 4th Workshop on Quantum Chaos and Localisation Phenomena, Warsaw 2009

Scattering Properties of Chaotic Microwave Billiards

H.-J. Stöckmann

Fachbereich Physik der Philipps-Universität Marburg, D-35032 Marburg, Germany

Reflection and transmission measurements in microwave billiards with attached antennas allow the determination of all components of the scattering matrix including their phases. This is an extraordinary situation, since in usual scattering experiments in nuclear or atomic physics only reduced information such as the scattering cross-section can be obtained where the phase information is completely lost. This allows experimental tests of theoretical predictions of scattering theory inaccessible by any other method. As an example the distribution of reflection coefficients and of the line widths in a chaotic microwave billiard are discussed.

PACS numbers: 03.65.Nk, 05.45.Mt

1. Introduction

In the spring times of nuclear physics in the midst of the last century there appeared a vast amount of experimental results on cross-sections, partial cross-section etc., obtained by bombarding target nuclei with light projectiles. In the interpretation of the spectra the physicists of that time faced two problems. First there was the task to separate the properties of the target nuclei from those of the projectiles. Taking the solution of this problem for granted, an even more severe one remained. Nearly nothing was known at that time on the origin of the nuclear forces. Could it be expected under such circumstances to obtain any relevant information at all from these irregularly looking spectra without any recognisable pattern?

The first of these two problems had been solved by the invention of scattering theory [1]. The scattering matrix S with its components S_{nm} connects the amplitudes $a_1, a_2, \ldots$ of the incoming "channels" with the amplitudes $b_1, b_2, \ldots$ of the outgoing "channels" via

$$b_n = \sum_m S_{nm} a_m. \tag{1}$$

In the context of nuclear physics the channels denote the incoming and outgoing particles such as protons, neutrons, deuterons etc., together with their respective momenta. In the case of microwave billiards to be discussed later the channels are just the attached antennas or waveguides.

Scattering theory establishes a relation between the experimentally obtainable scattering matrix S on one hand, and on the properties of the system under consideration on the other hand, which may be cast in the following form:

$$S = 1 - \mathrm{i}W^\dagger \frac{1}{E - H + \mathrm{i}WW^\dagger} W, \tag{2}$$

where H is the Hamilton operator of the unperturbed system, and W is a matrix containing the information on the coupling between the system and the channels. Truncating H to a finite rank N which is unavoidable in any theoretical treatment, W becomes a $N \times M$ matrix, where M is the number of attached channels.

Equation (2) shows that the scattering matrix is directly related to an effective Green function $G_{\mathrm{eff}} = (E - H_{\mathrm{eff}})^{-1}$, with the effective Hamiltonian $H_{\mathrm{eff}} = H - \mathrm{i}WW^\dagger$. The coupling to the channels enters thus in a twofold way. First, in the nominator, it couples the effective Green function to the channels, second, in the denominator, it gives rise to an imaginary part of the Hamiltonian, resulting in a broadening of the resonance lines. Equation (2) sometimes is called the "Heidelberg approach" since scattering theory had been developed in mayor parts by Weidenmüller and coworkers in Heidelberg [2].

The first problem being solved we now meet the second one: Nearly nothing had been known on the details of the Hamiltonian H, as well as on the elements of the coupling matrix W. How to proceed further in such an unfavourable situation? Here one idea showed up to be extremely useful, notwithstanding its obviously oversimplifying nature: If nothing is known on the matrix elements of H and W, just let us take them as random numbers, with only some global constraints, e.g. by taking the matrix H symmetric or Hermitian for systems with and without time-reversal symmetry, respectively, and by fixing the variance of the matrix elements of H and W. For technical reasons usually Gaussian distributed matrix elements are assumed [3].

With these assumptions a number of exact expressions for many quantities of interest can be calculated explicitly, such as spectral correlation functions, eigenvalue spacings distributions etc. The method of choice to calculate Gaussian averages is the supersymmetry technique. Unfortunately, the calculations are technically demanding already for comparatively simple questions, in particular for systems with time-reversal symmetry, being the most important ones. Again one of the most disseminating contributions in the field comes from Heidelberg called the VWZ report after the initials of its authors [4].

The replacement of H by a random matrix means to abandon any hope to learn more about nuclei from the

spectra but some average quantities such as the mean level spacings. Of course this is not the end of the story: there *are* techniques to extract also individual system properties, but this is not the topic of the present article. But the loss of individual features in the spectra on the other hand means that it might be worthwhile to look for *universal* features being common to all chaotic systems. This approach showed up to be extremely fruitful in the past years. It allowed to apply results originally obtained for nuclei to many other systems as well, in particular quantum–dot systems [5] and microwave billiards [6].

The latter systems had been studied by the author and his co-workers over many years starting with quantum chaos research, but concentrating in recent years on questions coming from scattering theory. A number of examples will be presented in this article. Microwave billiards have a number of advantages as compared to nuclei: (a) typical wavelengths are of the order of mm to cm, resulting in very convenient sizes for the used resonators, (b) sizes of the resonators, coupling strengths to antennas etc. can be perfectly controlled, (c) parameter variations, e.g. of the coupling strength of the size can be easily achieved, and (d) last but not least, in microwave systems the complete scattering matrix is obtainable, including the phases. This is extraordinary, since in nuclear physics usually only reduced information, such as scattering cross-sections is available, resulting in a complete loss of the phase information. This is why a number of predictions of scattering theory had been tested not in nuclei but microwave billiards.

This article is organised as follows: In Sect. 2 as an introductory example results on the distribution of reflection coefficients in a billiard with absorption are presented and compared with the predictions of scattering theory. Nearly all previous studies of this type concentrated on the study of such average quantities, where the knowledge of the poles of the scattering matrix (2) is not needed. The determination of these poles is simple as long as the resonances are separated. In the really interesting regime of strong overlap, however, this had been not achieved until recently, apart from one exception from our group. Here a breakthrough appeared by the adoption of the method of harmonic inversion to determine the poles of the scattering matrix. As this technique is not yet familiar to everybody, its essentials are explained in Sect. 3. In the last Sect. 4 the method is applied to microwave spectra, extending the determination of the poles up to the regime where the line widths amount to up to ten times the mean level spacings. The presentation in the following sections is deliberately colloquial and omits all technical details. The reader is referred to the original works for more information.

2. Distribution of reflection coefficients

Because of the difficulty to resolve the poles of the scattering matrix in the regime of strong overlap, most studies, both experimentally and theoretically, concentrated on quantities, where an explicit knowledge of these poles is not needed such as the distribution of reflection and transmission coefficients, as well as various types of spectral correlation functions [7–11], see Ref. [12] for a review. As a typical example of this kind we present here a study of the distribution of reflection coefficients as a function of absorption [7]. Figure 1 shows the used setup. The studied system had been a quasi-two-dimensional resonator of the shape of a half Sinai billiard, one of the paradigms of classical non-linear dynamics. The resonator had been quasi-two-dimensional, i.e., with top and bottom plate parallel to each other and a height smaller than half of the wave length. In such systems there is a complete equivalence to the quantum mechanics of the corresponding billiard system with Dirichlet boundary conditions. In part of the measurements one of the walls had been coated by absorbing material to increase the absorption. The microwave field had been excited by one antenna, used also for the reflection measurement.

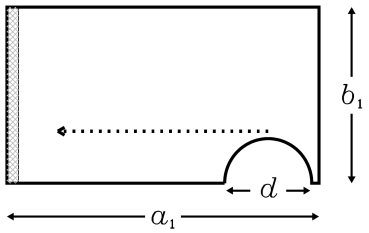

Fig. 1. Sketch of the used microwave billiard (a_1 = 43 cm, b_1 = 23.7 cm, height h_1 = 7.8 mm). The half disk (d = 12 cm) could be moved along a_1 to allow for an ensemble average. In part of the measurements one wall was coated with an absorber (taken from Ref. [7]).

Figure 2 shows typical reflection spectra for three different regimes. The spectrum of Fig. 2a has been obtained in the low frequency regime, where all resonances are well resolved. This regime is well understood [13]. Here for the reflection $R = S_{11}$ relation (2) reduces to

$$R = 1 - 2\mathrm{i}\gamma \sum_k \frac{|\psi_k(r)|^2}{E - E_k + \mathrm{i}\Gamma_k}, \tag{3}$$

where γ is a coupling constant depending on the antenna properties, E_k is the energy of the k-th eigenstate, and Γ_k is the width of this state due to the antenna coupling. Equation (3) is the billiard equivalent of the Breit–Wigner formula known from nuclear physics for decades. Since all theories have been developed for quantum-mechanical systems, in Eq. (3) the quantum-mechanical expression for the reflection has been given. The corresponding electromagnetic expression looks slightly different, resulting from the different dispersion relations $\omega \sim k^2$ and $\omega \sim k$ for quantum-mechanical and electromagnet systems, respectively (see Ref. [12] for details).

Figure 2b has been obtained for the same system, but for higher frequencies. Since in two-dimensional systems the density of states increases proportionally to k, the ratio of the mean level spacings Δ to the mean line width Γ decreases with frequency resulting in an increas-

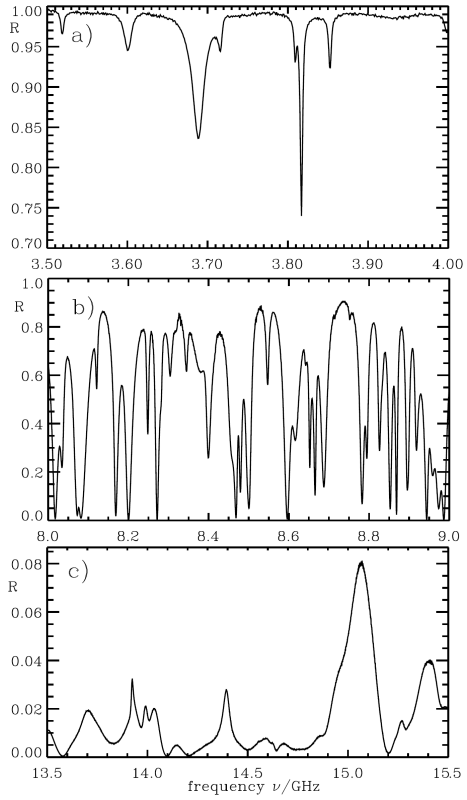

Fig. 2. Typical absorption spectra for the Sinai billiard shown in Fig. 1 for weak (a), intermediate (b), and strong (c) absorption. The results for weak and intermediate absorption have been obtained without the absorber at one of the walls, for the strong absorption the absorber had been present (taken from Ref. [7]).

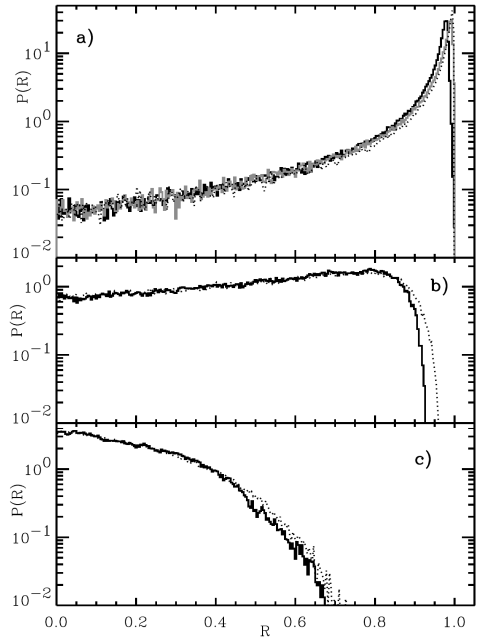

Fig. 3. Distribution of reflection coefficients for (a) weak, (b) intermediate and (c) strong absorption, obtained for the same regimes as in Fig. 2. The solid lines are the experimental results, the dotted lines are the result of a simulation (taken from Ref. [7]).

ing overlap of resonances with increasing frequency. In this regime individual resonances cannot be resolved any longer, and only chaotic fluctuations are observed. In nuclear physics the corresponding features are the well--known Ericson fluctuations discovered in the sixties of the last centuries. About 20 years later the same features have been found in the transport through quantum-dot structures, where they have been termed "universal conductance fluctuations". And now we see the same fluctuations again in microwave billiards! This illustrates the charm of the universal approach: The physical properties of the three mentioned systems are completely different, and their sizes extend over 15 orders of magnitude, but still the theoretical treatment is the same.

These measurements had been obtained with the billiard shown in Fig. 1 without the additional absorber. To increase the absorption even more, the absorber had been inserted. As a result only very broad, purely resolved structures appeared, see Fig. 2c. This limit again is well understood [14].

Figure 3 shows the reflection distributions $p(R)$ for the same three regimes which had been selected in Fig. 2. At the time, when the measurements had been performed, theoretical results for $p(R)$ in the presence of absorption had been available only in the weak [13] and the strong [14] absorption limit, but not in between. Therefore the experimental distributions had been compared with the results of random matrix simulation, using the Heidelberg expression (2) for the scattering matrix, and taking Gaussian averages over all occurring matrix elements. There had been only two free parameters namely the coupling constant γ of the antenna and the average absorption. Both parameters had been determined directly from the experimentally available averages of the absorption and the reflection. These parameters had been used in the simulation leaving no adjustable parameter. Nevertheless a nearly perfect agreement between experiment and simulation is found, justifying the random matrix treatment of the microwave billiard.

Motivated by the experiments our theoretical colleagues meanwhile managed to find an explicit analytical expression for $p(R)$ covering the whole range from weak to strong absorption [15]. Again the agreement was perfect, both with the experiment and the simulations.

3. The harmonic inversion technique

For average quantities such as the distribution of reflection coefficients knowledge of the pole structure of the scattering matrix is not needed. The same is true for most previous experiments on reflection and transmission properties of chaotic microwave billiards and graphs. There had been only one previous study performed in the

author's lab where the dynamics of the poles in the complex plane could be followed in dependence of the opening of an attached channel [16]. The experiments exhibited the phenomenon of resonance trapping, i.e., the feature that with increasing opening most poles do not separate more and more from the real axis but eventually return again. This had been the first and hitherto only experimental observation of this, at first sight, counterintuitive behaviour. To come to this result, a standard fit procedure was still feasible. But it was limited to regimes where the mean line width Γ amounted to at most four to five times the mean level spacing Δ, and is definitely not suited as a standard tool to analyse resonances in the regime of strong overlap.

Here the method of harmonic inversion poses an alternative. It has been introduced by Wall and Neuhauser [17] and further developed by Mandelshtam and Taylor [18], but it was Main who brought the codes into a manageable form suited for the application to experimental data [19]. Since the technique is not yet sufficiently well known, the essentials of the method are presented here in a cursory form. The following presentation follows the paper by Wiersig and Main [20].

The harmonic inversion is capable to extract the number of resonances hidden in a measured spectrum without any foreknowledge on its number. This is a huge advantage as compared to standard fit procedures. As an input the method needs a complex signal on the time axis being a superposition of exponentially damped oscillations

$$c(t) = \sum_{k=1}^{K} d_k \, \mathrm{e}^{-\mathrm{i}\omega_k t}, \quad \omega_k = \Omega_k - \frac{\mathrm{i}}{2}\Gamma_k. \tag{4}$$

Discretising the time in finite steps for τ one gets

$$c_n = c(n\tau) = \sum_{k=1}^{K} d_k \, (z_k)^n \,, \quad z_k = \mathrm{e}^{-\mathrm{i}\omega_k \tau}. \tag{5}$$

Applying a discretised Mellin transform and summing up the resulting geometric series one obtains

$$g(z) = \sum_{n=0}^{\infty} c_n z^{-n} = \sum_{k=1}^{K} d_k \sum_{n=0}^{\infty} \left(\frac{z_k}{z}\right)^n = \sum_{k=1}^{K} \frac{z d_k}{z - z_k}. \tag{6}$$

Let us note that this approach assumes an extrapolation of the time signal over arbitrarily long times. It can therefore work for time signals only where there is no doubt that the time series really can be written as a sum over damped oscillatory terms. The latter expression can be written as

$$g(z) = \frac{P_{\mathrm{K}}(z)}{Q_{\mathrm{K}}(z)}, \tag{7}$$

where $P_K(z), Q_K(z)$ are polynomials of degree K, the number of term in the sum (6). The z_k are the zeros of $Q_K(z)$, and the d_k are obtained by the residuum method as $d_k = P_K(z_k)/[z_k Q'_{\mathrm{K}}(z_k)]$. And now crucial point: Knowledge of $2K$ signal points $c_0, \ldots, c_{2K-1}$ is sufficient to calculate the coefficients of the two polynomials,

$$P_K(z) = \sum_{k=1}^{K} b_k z^k, \quad Q_{\mathrm{K}}(z) = \sum_{k=1}^{K} a_k z^k - 1. \tag{8}$$

First the coefficients a_k of $Q_K(z)$ obtained as solutions of the linear set of equations

$$c_n = \sum_{k=1}^{K} c_{n+k} a_k, \quad n = 0, \ldots, K-1. \tag{9}$$

Let us note that the c_n obtained from the discretization of the time signal enter in two different ways, on the left hand side in terms of a vector, on the right hand side in terms of a matrix. Once the a_k are known, the coefficients b_k of $P_K(z)$ are obtained from

$$b_k = \sum_{m=0}^{K-k} a_{k+m} c_m, \quad k = 1, \ldots, K. \tag{10}$$

Next the z_k are determined as the zeros of $Q_K(z)$. One convenient way to do this is to interpret $Q_K(z)$ as the characteristic polynomial of some matrix, the eigenvalues of which can be obtained by standard techniques. In the last step the d_k are obtained by the residuum technique, see above.

Since the experimental spectra have been taken on the frequency axis, first of all they have to be converted to the time domain by means of a Fourier transform. From scattering theory we know that any reflection signal can be written as

$$R(E) = 1 - \sum_k \frac{d_k}{E - E_k}, \tag{11}$$

where the E_k are the (complex) zeros of H_{eff}, see Eq. (2), and the d_k are the respective residua. Again the quantum-mechanical description has been applied to be in accordance with the notation of Sect. 1. After Fourier transforming Eq. (11) we obtain the wanted time signal

$$\hat{R}(t) = \delta(E) - \sum_k d_k \, \mathrm{e}^{-\mathrm{i}\omega_k t} \tag{12}$$

with $\omega_k = E_k/\hbar = \Omega_k - \mathrm{i}\,\Gamma_k$.

The application of the Fourier transform assumes that there are no other energy dependences apart from those occurring in the poles of the scattering matrix. In real experimental data this is not strictly true. The coupling of the antennas is energy dependent, too, though usually only slowly varying with energy. In the Fourier transform these additional energy dependences map into non-exponential contributions to the decay of the signal. The harmonic inversion tries to describe these additional terms in terms of a superposition of exponentials giving rise to an unwanted background.

The signal (12) can now be treated by the harmonic inversion technique. The rank K of the matrices constructed from the time signal is not needed for this purpose. It is sufficient to take a value exceeding the number of expected resonances. To this end the number of values c_k must exceed K by a factor of two, an obvious condition, since each resonance is characterised by two parameters ω_k, d_k. In the end one faces the problem to distinguish between real and spurious resonances. There

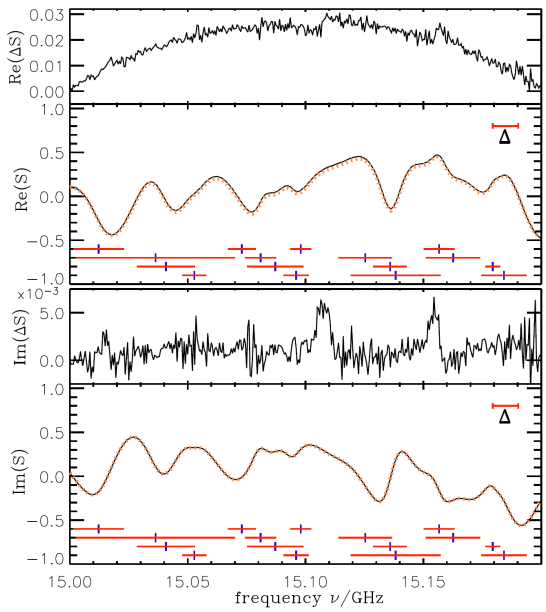

Fig. 4. Real and imaginary part of a part of the spectrum in the regime of overlapping resonances. Additionally the reconstructed spectrum using the resonances identified by the harmonic inversion is shown in dashed. The vertical lines indicate the positions of the resonances and the horizontal lines the corresponding widths at half maximum. On top of each figure the difference between the measured spectrum and the calculated one is shown. The mean level spacing Δ is marked by a horizontal bar (taken from Ref. [12]).

are a number of options, e.g., introducing cut-off criteria for d_k, varying the starting point of the time series, using different windows and window functions for the Fourier transform etc.

Figure 4 shows, how the method works [21]. The solid lines in the upper and the lower part show real and imaginary part of a part of the spectrum of the Sinai resonator in Fig. 1 in the regime of intermediate overlap. The same data set had been used for the determination of the reflection distribution discussed in Sect. 2. The resonances obtained by harmonic inversion and surviving a couple of cut-off tests are depicted below, where the dots denote the position of the resonance and the vertical bars their width. The dashed line is the reconstructed signal using the surviving resonances found in the harmonic inversion. In the upper parts of the figures the difference between the original and the reconstructed signal is shown illustrating the quality of the technique. To come to such a good agreement, it was necessary to subtract a linear background from the reconstructed signal such that both original and reconstructed signal coincide at the lower and the upper frequencies of the window displayed in the figure. This background has its origin in the additional frequency dependences in the antenna coupling mentioned above.

In the present case the number of expected resonances in the shown frequency window can be calculated from the Weyl formula and should be 18, whereas the number of found resonances is 16. In fact the two missing resonances show up in the difference between the original and the reconstructed spectra at 15.11 and 15.15 GHz. They just did not survive the applied cut-off criteria. Here we see the limitation of the method: without further information (spectral level dynamics, use of more than just one antenna position etc.) one always will lose the one or the other true resonance, and at the same time will misinterpret noise peaks as real resonances. Since this had been the first application of the harmonic inversion to experimental data, a longer-term experience will be needed to explore the limits of the technique in this respect.

4. Line width distributions

The possibility to analyse the poles of the scattering matrix even for strongly overlaping resonances opens the possibility to study questions hitherto not accessible by the experiment [21]. As an example Fig. 5 shows the result of the harmonic inversion to the spectrum of the billiard shown in Fig. 1 in the intermediate regime. Only a subset of the poles is shown in the main figure. A better impression of what can be achieved can be obtained from the inset where all found resonances were depicted. The dashed line close to the real axis corresponds to the line width expected from wall absorption due to the skin effect. One sees that this is only a minor contribution to the total line width. The dashed line corresponds to the average absorption obtained if the decay of the scattering matrix on the time axis is fitted by an exponential. The strong scattering of the poles about this average value shows that the assumption of just one exponential decay is not justified, which had not been such obvious from a mere look into the decay of the scattering matrix.

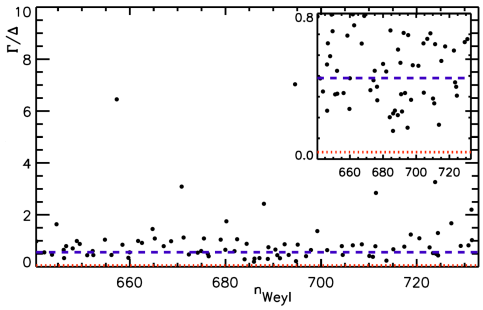

Fig. 5. Normalized widths Γ/Δ for 14.7 to 15.7 GHz. The horizontal dashed line corresponds to the width coming from the total absorption, whereas the dotted line (only visible in the inset) corresponds to the constant part of the absorption. The inset is an enlargement of the small width region (taken from Ref. [12]).

The most obvious quantity to look at is the distribution of line widths. Here an analytic result has been obtained for an arbitrary number of coupled channels by Sommers et al. [22, 23], but the formulae are "rather awkward even for the simplest case" (literally cited from the

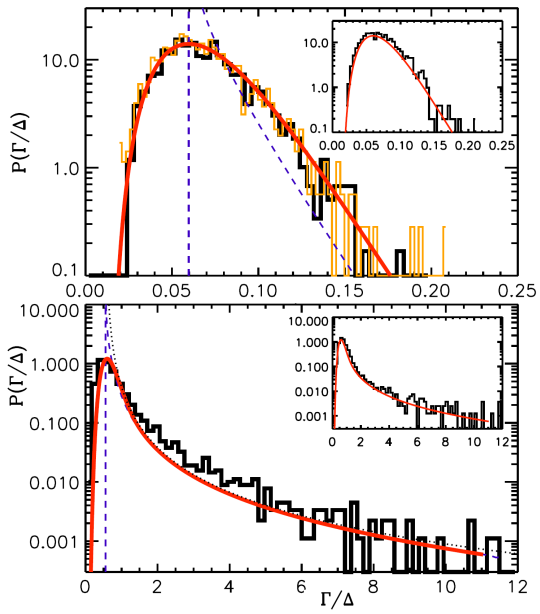

Fig. 6. Normalized width distribution in the frequency range 4 to 5 GHz (top) and 14.7 to 15.7 GHz (bottom). The black histograms had been obtained from the harmonic inversion, the light (gray) one in the upper figure from a Lorentzian fitting procedure of the isolated resonances. The dashed curves correspond to the theoretical prediction from Eq. (14) shifted by a constant off-set to account for absorption in the walls. The solid line in addition takes into account the fluctuations caused by additional weakly coupled channels. The insets show the results of a random matrix simulation using the same values for antenna coupling etc. as in the experiment (taken from Ref. [12]).

original work). For the one-channel case in particular one obtains for the line width distribution

$$P(y) = \frac{1}{4}\frac{\partial^2}{\partial y^2}\int_{-1}^{1} \mathrm{d}\lambda(1-\lambda^2)\,\mathrm{e}^{2\pi\lambda y}F(\lambda,y),$$
$$y = \Gamma/\Delta. \qquad (13)$$

$y = \Gamma/\Delta$ is the line width in units of the mean level spacings, and

$$F(\lambda,y) = (g-\lambda) \times \int_g^\infty \mathrm{d}p_1 \frac{\mathrm{e}^{-\pi y p_1}}{(\lambda-p_1)^2\sqrt{(p_1^2-1)(p_1-g)}} \times \int_1^g \mathrm{d}p_2 \frac{(p_1-p_2)\,\mathrm{e}^{-\pi y p_2}}{(\lambda-p_2)^2\sqrt{(p_2^2-1)(g-p_2)}}. \qquad (14)$$

g is a constant describing the antenna coupling. $g = 1$ corresponds to an ideally coupled channel, whereas in the limit $g \to \infty$ the coupling vanishes. In Fig. 6 the experimentally obtained line width distributions are compared with theory in the regime of isolated and strongly overlapping resonances (see Fig. 2a and c). In the aforementioned case it was still possible to determine the resonances by standard fit procedures. The results are in perfect agreement with those obtained by harmonic inversion. In the strongly overlapping case any trial to determine the resonance by a multi-line fit would have been hopeless from the very beginning. The dashed lines correspond to the line width distribution (14), where in addition a constant overall line width distribution due to wall absorption has been assumed. The overall absorption and the coupling had been determined independently (see Sect. 2), thus there are no free parameters. One finds a good agreement in the regime of strongly overlapping resonances. Let us note that this agreement is observed up to the regime where the line width exceeds the mean level spacing by up to a factor of 10! For the isolated resonance, however, there is obviously something missing.

The origin of this discrepancy is easily identified: it is the assumption of a uniform general absorption giving the same constant line width contribution to all resonances. If one assumes instead that there is a small number of weakly coupled channels, 10 of them in the isolated resonance and 20 in the strongly overlapping regime, a nearly perfect correspondence between experiment and theory is obtained.

5. Conclusions

In the present paper only one, though central, aspect of the microwave experiments has been discussed, namely the interpretation of microwave billiards in terms of a scattering system. It has been shown that there is no essential difference to other scattering systems such as atoms, nuclei, or quantum dots, as long as only universal features are concerned.

Whereas in the past only average quantities could be studied such as the distribution of reflection coefficients, thanks to the application of the harmonic inversion technique now the pole structure of the scattering matrix can be resolved even in the regime of strong overlap, having been a dream for many years. The determination of the line width distribution means only a first step towards the exploration of the complex plane. Many other issues of interest are now accessible, such as eigenvalue distance distributions in the complex plane, or the extension of spectral level dynamics studies to the complex plane, to mention just two issues.

Acknowledgments

All experiments and data analysis presented in this article have been performed by my co-workers. In particular I would like to mention U. Kuhl who cared for the harmonic inversion analysis of the spectra. J. Main, Stuttgart, Germany, brought in his expertise on the harmonic inversion technique and provided the necessary computer codes. The study of the distribution of reflection coefficients had been performed by R. Méndez-Sánchez, Cuernavaca, Mexico, during several visits in Marburg. All this is gratefully acknowledged. Last

but not least I would like the Deutsche Forschungs--Gemeinschaft for their support of the experiments beneath the roof of the research group 760 "Scattering systems with complex dynamics".

References

[1] C. Mahaux, H.A. Weidenmüller, *Shell-Model Approach to Nuclear Reactions*, North-Holland, Amsterdam 1969.

[2] T. Guhr, A. Müller-Groeling, H.A. Weidenmüller, *Phys. Rep.* **299**, 189 (1998).

[3] M.L. Mehta, *Random Matrices*, 2nd ed., Academic Press, San Diego 1991.

[4] J.J.M. Verbaarschot, H.A. Weidenmüller, M.R. Zirnbauer, *Phys.] Rep.* **129**, 367 (1985).

[5] C.W.J. Beenakker, *Rev. Mod. Phys.* **69**, 731 (1997).

[6] H.-J. Stöckmann, *Quantum Chaos — An Introduction*, University Press, Cambridge 1999.

[7] R.A. Méndez-Sánchez, U. Kuhl, M. Barth, C.H. Lewenkopf, H.-J. Stöckmann, *Phys. Rev. Lett.* **91**, 174102 (2003).

[8] H. Schanze, E.R.P. Alves, C.H. Lewenkopf, H.-J. Stöckmann, *Phys. Rev. E* **64**, 065201(R) (2001).

[9] S. Hemmady, X. Zheng, E. Ott, T.M. Antonsen, S.M. Anlage, *Phys. Rev. Lett.* **94**, 014102 (2005).

[10] O. Hul, O. Tymoshchuk, S. Bauch, P. Koch, L. Sirko, *J. Phys. A* **38**, 10489 (2005).

[11] J. Barthélemy, O. Legrand, F. Mortessagne, *Phys. Rev. E* **71**, 016205 (2005).

[12] U. Kuhl, H.-J. Stöckmann, R. Weaver, *J. Phys. A* **38**, 10433 (2005).

[13] P.W. Brouwer, C.W.J. Beenakker, *Phys. Rev. B* **50**, 11263 (1994).

[14] E. Kogan, P.A. Mello, H. Liqun, *Phys. Rev. E* **61**, R17 (2000).

[15] Y.V. Fyodorov, D.V. Savin, *JETP Lett.* **80**, 725 (2004).

[16] E. Persson, I. Rotter, H.-J. Stöckmann, M. Barth, *Phys. Rev. Lett.* **85**, 2478 (2000).

[17] M.R. Wall, D. Neuhauser, *J. Chem. Phys.* **102**, 8011 (1995).

[18] V.A. Mandelshtam, H.S. Taylor, *J. Chem. Phys.* **107**, 6756 (1997).

[19] J. Main, *Phys. Rep.* **316**, 233 (1999).

[20] J. Wiersig, J. Main, *Phys. Rev. E* **77**, 036205 (2008).

[21] U. Kuhl, R. Höhmann, J. Main, H.-J. Stöckmann, *Phys. Rev. Lett.* **100**, 254101 (2008).

[22] H.J. Sommers, Y.V. Fyodorov, M. Titov, *J. Phys. A* **32**, L77 (1999).

[23] Y.V. Fyodorov, D.V. Savin, H.-J. Sommers, *J. Phys. A* **38**, 10731 (2005).